2021 43rd Annual International Conference of the
IEEE Engineering in Medicine & Biology Society (EMBC)
Oct 31 - Nov 4, 2021. Virtual Conference

Radiofrequency heating of retained cardiac leads during magnetic resonance imaging at 1.5 T and 3 T

Bach T. Nguyen, Bhumi Bhusal, Kate Fawcett, and Laleh Golestanirad, *Member, IEEE*

***Abstract*— Patients with cardiovascular implantable electronic devices (CIEDs) are often prevented from receiving magnetic resonance imaging (MRI) due to risks associated with radiofrequency (RF) heating of tissue around the implanted leads. Although MR-conditional CIEDs are available, the safety labeling of such devices does not extend to patients with fragmented retained leads (FRLs), where segments of the leads are left in the tissue after the original device is extracted. Unlike intact and isolated leads of CIEDs, FRLs are often bare conductive lead fragments in direct contact with the tissue. No experimental work has been reported that assess RF heating of FRL during MRI thus far. In this work, we performed phantom experiments to measure RF heating of 4 patient-derived FRL models in a gel-based ASTM-like phantom during RF exposure at 64 MHz (proton imaging at 1.5 T) and 123 MHz (proton imaging at 3 T). We found FRL models to generate negligible temperature rise in the gel (ΔT<1.84 °C) during a 10-minute scan at both 1.5 T and 3 T. These results are in agreement with previous simulation studies and suggest MRI may be performed safely in patients with fragmented retained leads.**

I. Introduction

With an aging population and occurrence of more significant cardiac disease, cardiovascular implantable electronic devices (CIEDs) are used more frequently. Many studies have assessed safety of magnetic resonance imaging (MRI) in patients with intact CIED leads connected to working devices. Some patients, however, require the leads to be extracted due to technical failure which usually leaves fractions of the lead *in situ* as complete lead removal is not always possible [1]. This leaves a sizeable cohort of patients with fragmented retained leads (FRLs) [2, 3] to which the original MRI safety assessment does not apply anymore and studies that assess safety of MRI in patients with CIEDs mostly exclude those with FRLs [1, 4].

In a previous simulation study, we reported the specific absorption rate (SAR) of the radiofrequency (RF) energy deposited in the tissue surrounding FRL models in a homogenous body model [5]. Based on the simulated temperature rise in the tissue surrounding the leads, the study concluded that MRI may be performed safely in patients ($\Delta T < 6$ °C) as long as the RF magnetic field (B_1^+) remained below 4 μT at 1.5 T and below 2 μT at 3 T. These results, however, have not been experimentally verified.

Here we report, for the first time, results of an experimental study measuring RF heating of FRL models implanted in an ASTM phantom during MRI RF exposure at 64 MHz and 123 MHz (proton imaging at 1.5 T and 3 T). We created models of FRLs from commercially available pacemaker leads (Medtronic 5076), with trajectory/geometries mimicking those observed in radiographic images of patients with CIEDs. We measured temperature rise around the leads in a tissue mimicking gel during 10 minutes of RF exposure at 1.5 T and 3 T. The maximum temperature rise in the gel was recorded to be 1.84 °C which occurred at the lead's tip. Our results confirm previous simulations, suggesting that MRI at 1.5 T and 3 T may be performed safely in patients with FRLs. This is also in agreement with recent studies that reported lack of adverse effects in patients with FRLs who underwent MRI [6].

II. Methods

A. Creation of FRL models

It is well established that the trajectory and position of an elongated conductive lead substantially affects its MRI-induced RF heating [7-15]. For this reason, it is important to assess RF heating of retained leads using FRL models with clinically relevant trajectories. To do this, we inspected chest CT and X-ray images of patients with a history of implanted cardiac devices who had been admitted to Northwestern Memorial Hospital between 2006 and 2018. From patients identified with FRLs, 4 patients who had images that clearly delineated the FRL trajectory were included in the study (Figure 1). FRL trajectories were segmented from CT images using Amira software (Thermo Fisher Scientific, Waltham MA) following steps similar to what is described in our previous work [16]. In brief, we applied a thresholding algorithm based on an intensity histogram analysis which extracted a preliminary mask of the hyper-dense FRL from the CT image. 3D lead surfaces were exported to a CAD tool (Rhino3D, Robert McNeal and Associates, Seattle, WA) in which trajectory lines were manually extracted, thickened, and prepared for 3D printing. Trajectory guides were 3D printed out of polycarbonate plastic and used to shape internal conductive wires of Medtronic 5076 leads to replicate FRL models with trajectories mimicking those observed in patients. Figure 1 shows steps of image segmentation and model preparation.

B. MRI exposure setup

Experiments were performed using a Siemens Aera 1.5 T and Siemens Prisma 3 T scanners (Siemens Healthineers, Erlangen, Germany). FRL models were immersed in an ASTM phantom filled with a gel prepared by mixing 10 g/l of

*Research supported by National Institute of Health grant R03EB025344.

B.T. Nguyen, B. Bhusal, and K. Fawcett are with the Department of Radiology, Northwestern University Chicago, IL 60611 USA.

Corresponding Author: L. Golestanirad is with the Department of Radiology and Department of Biomedical Engineering, Northwestern University, Chicago, IL, 60611 USA. Email: laleh.rad1@northwestern.edu.

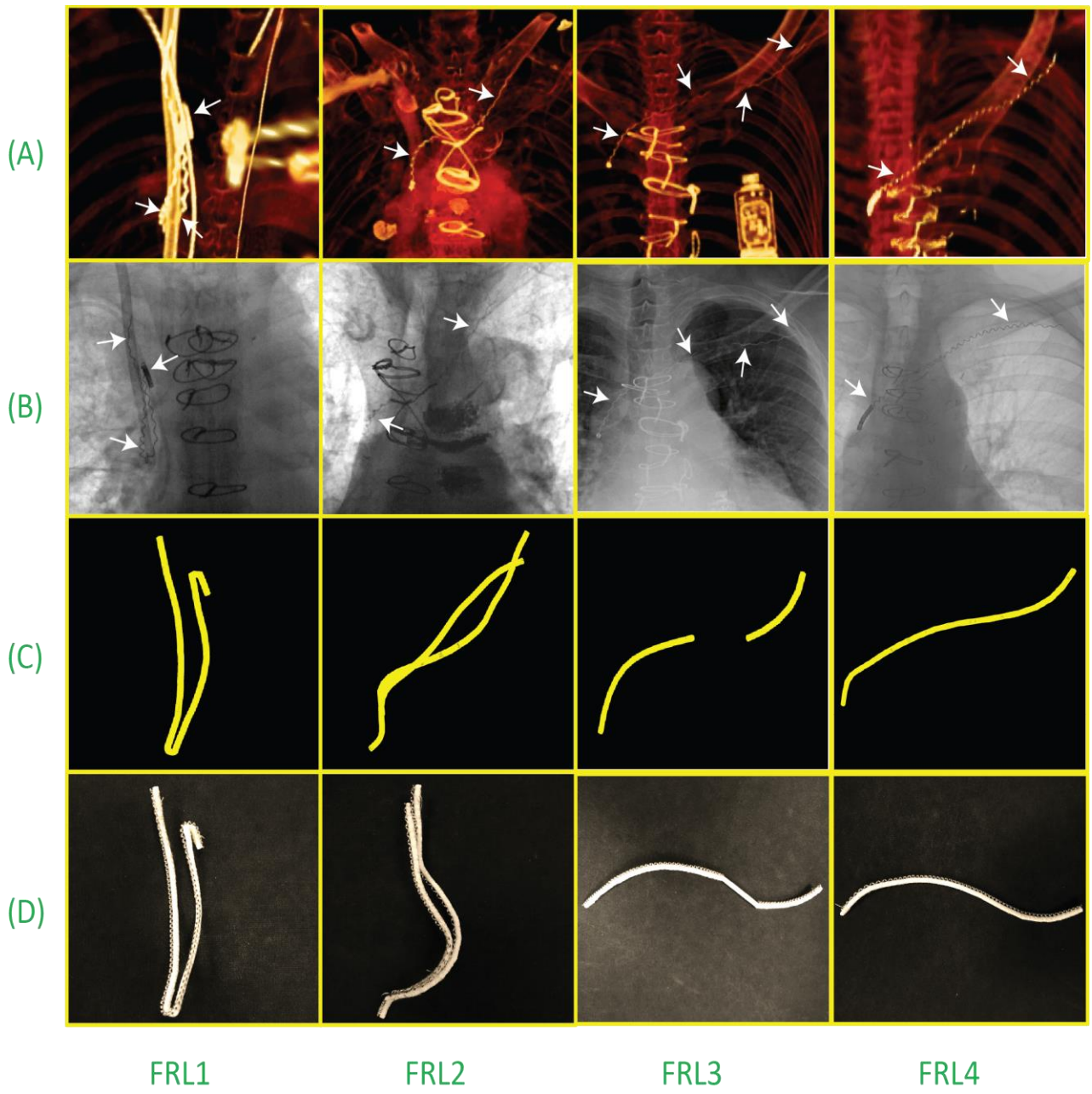

Figure 1. Image segmentation and model construction. (A-B) CT and X-ray images were used to extract the 3D lead trajectories, (C) reconstructed trajectories, (D) 3D printed plastic guides attached to lead fragments.

Polyacrylic Acid (PAA, Aldrich Chemical) and 1.32 g/l Sodium Chloride into distilled water. Bulk conductivity and relative permittivity of the gel was measured to be $\sigma = 0.46$ S/m and $\varepsilon_r = 87.7$, using a dielectric probe kit (85070E, Agilent Technologies, Santa Clara, CA) and a network analyzer. FRL models were positioned in a location analogous to middle of the chest similar to what we observed in patient images. Two fluoroptic temperature probes (OSENSA, BC, Canada) were secured at both tips for all FRL models, while one additional probe was attached at the middle of the FRL1 and FRL3 models, where the FRL1 lead has a bent shape and the FRL3 was broken into two separated parts. Temperature rise ΔT in the gel was recorded during 10 minutes of RF exposure using a high-SAR T1-turbo spin echo (T1-TSE) sequence (TE = 7.3 msec, TR = 814 msec, flip angle = 150°, $B_1^+ = 4.1$ μT for 1.5 T scans; and TE = 7.5 msec, TR = 1450 msec, flip angle = 150°, $B_1^+ = 2.8$ μT for 3 T scans). The sequence parameters were adjusted to generate the maximum SAR allowed by the scanner to assess the worst-case heating scenario.

Imaging was performed using scanner's built-in body coil. The ASTM phantom was positioned such that the chest was at the coil's iso-center. This position was shown to generate the highest heating in simulations [5]. Figure 2 shows details of the experimental setup.

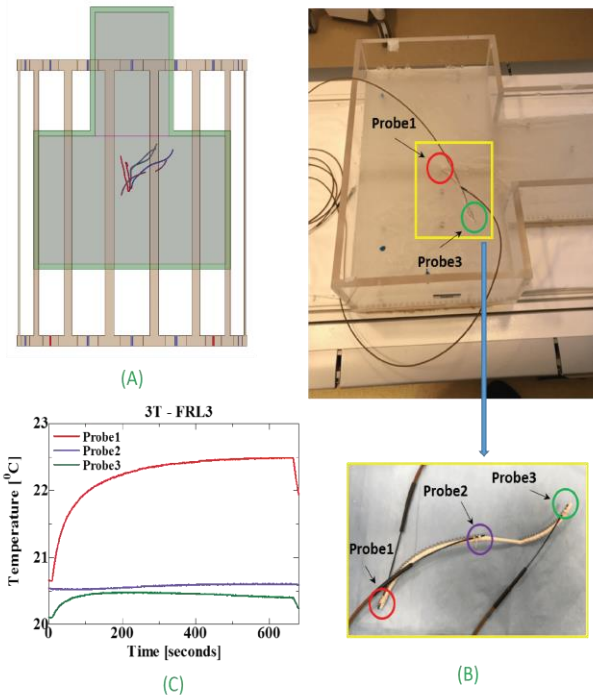

Figure 2. (A) the location of 4 FRL models inside the phantom and the positioning of the phantom inside the body coil, (B) the experimental setup for FRL3 and the positions of temperature probes, and (C) their temperature responses at 3 T.

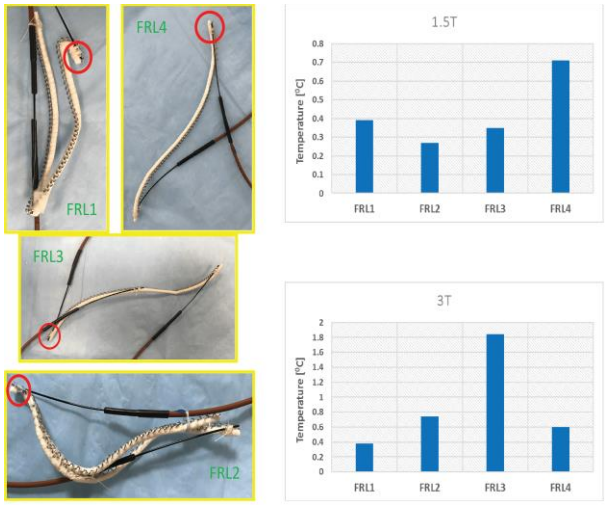

Figure 3. Comparison of highest temperature rises of FRL models at 1.5 T and 3 T, as well as the locations where the maximum temperatures were measured.

III. Results

Figure 2C shows an example of the temporal profile of the temperature rise in the gel measured at 3 probes positioned at two ends and at the middle of the FRL3 model at 3 T during a 10-minute scan. The temperature rise at one of the lead's tip (Probe 1) was significantly higher than the temperature rise at the other tip (Probe 3), while we observed negligible heating at the midpoint (Probe 2).

Figure 3 shows the highest temperature rise observed for each FRL along with their location marked by red circles. The maximum temperature rise was 1.84 °C measured at the tip of FRL3 model during MRI at 3 T.

IV. Discussion and Conclusion

Efforts to develop MRI-compatible CIEDs are recent, with newly approved devices allowing conditional MRI of patients with intact cardiac leads at both 1.5 T and 3 T scanners. There is, however, a sizeable cohort of patients with abandoned or retained leads for whom MRI under current labeling is an absolute contraindication, mostly because little is known about the phenomenology of MRI-induced heating in the tissue in the presence of partially extracted leads. The major challenge in quantifying implant-induced heating in this case is that the problem has a large parameter space with many variables that interact with each other. This includes the frequency and geometry of MRI RF coil, the length, trajectory, and structure of the abandoned/retained lead, the imaging landmark, and the patient's anatomy. Such complexity precludes the application of a systematic experimental approach to infer the worst-case heating scenario.

Our previous work established the first simulation study of MRI hazards in patients with fragmented retained leads (FRLs) with a focus on RF heating [5]. This study provides the first experimental-based safety assessment of MRI at 1.5 T and 3 T in patients with fragmented retained leads.

The maximum temperature rise was measured to be <2 °C at 3 T and < 1 °C at 1.5 T. In general, higher heating was observed at 3 T compared to 1.5 T, which is consistent with previous simulation results [5]. This observation was interesting considering that in this experimental study, the B_1^+ at 3 T was smaller than B_1^+ at 1.5 T due to scanner-imposed SAR limitation. Our results suggest that the FRLs might not produce excessive heating during MRI at both 1.5 T and 3 T. However, more comprehensive studies with additional FRL models under variant imaging conditions and tissue properties are required to make a general conclusion about the safety of such leads during MRI.

Acknowledgment

This work has been supported by NIH grant R03EB025344.

References

[1] L. Holzhauser *et al.*, "Consequences of Retained Defibrillator and Pacemaker Leads After Heart Transplantation—An Underrecognized Problem," *Journal of cardiac failure,* vol. 24, no. 2, pp. 101-108, 2018.

[2] A. Martin, J. Voss, D. Shannon, P. Ruygrok, and N. Lever, "Frequency and sequelae of retained implanted cardiac device material post heart transplantation," *Pacing and Clinical Electrophysiology,* vol. 37, no. 2, pp. 242-248, 2014.

[3] A. Koshy, S. Nanayakkara, D. McGiffin, J. Martin, P. Bergin, and J. Mariani, "Retained defibrillator leads following orthotopic heart transplantation," *International journal of cardiology,* vol. 215, pp. 87-89, 2016.

[4] R. J. Russo *et al.*, "Assessing the risks associated with MRI in patients with a pacemaker or defibrillator," *New England Journal of Medicine,* vol. 376, no. 8, pp. 755-764, 2017.

[5] L. Golestanirad *et al.*, "Changes in the specific absorption rate (SAR) of radiofrequency energy in patients with retained cardiac leads during MRI at 1.5 T and 3T," *Magnetic resonance in medicine,* vol. 81, no. 1, pp. 653-669, 2019.

[6] C. O. Austin, K. Landolfo, P. P. Parikh, P. C. Patel, K. Venkatachalam, and F. M. Kusumoto, "Retained cardiac implantable electronic device fragments are not associated with magnetic resonance imaging safety issues, morbidity, or mortality after orthotopic heart transplant," *American heart journal,* vol. 190, pp. 46-53, 2017.

[7] L. Golestanirad, L. M. Angelone, M. I. Iacono, H. Katnani, L. L. Wald, and G. Bonmassar, "Local SAR near deep brain stimulation (DBS) electrodes at 64 and 127 MH z: A simulation study of the effect of extracranial loops," *Magnetic resonance in medicine,* vol. 78, no. 4, pp. 1558-1565, 2017.

[8] L. Golestanirad *et al.*, "RF-induced heating in tissue near bilateral DBS implants during MRI at 1.5 T and 3T: The role of surgical lead management," *NeuroImage,* vol. 184, pp. 566-576, 2019.

[9] C. McElcheran *et al.*, "Numerical simulations of realistic lead trajectories and an experimental verification support the efficacy of parallel radiofrequency transmission to reduce heating of deep brain stimulation implants during MRI," *Scientific reports,* vol. 9, no. 1, pp. 1-14, 2019.

[10] B. Bhusal *et al.*, "Effect of device configuration and patient's body composition on nonsusceptibility artifact and RF heating of deep brain stimulation devices during MRI at 1.5 T and 3 T," *Journal of Magnetic Resonance Imaging* vol. 53, no. 2, pp. 599-610, 2021.

[11] B. T. Nguyen, J. Pilitsis, and L. Golestanirad, "The effect of simulation strategies on prediction of power deposition in the tissue around electronic implants during magnetic resonance imaging," *Physics in Medicine & Biology*, vol. 65, no. 18, p. 185007, 2020.

[12] B. Bhusal, B. Keil, J. Rosenow, E. Kazemivalipour, and L. Golestanirad, "Patient's body composition can significantly affect RF power deposition in the tissue around DBS implants: ramifications for lead management strategies and MRI field-shaping techniques," *Physics in Medicine & Biology*, vol. 66, no. 1, p. 015008, 2021.

[13] L. Golestanirad et al., "Variation of RF heating around deep brain stimulation leads during 3.0 T MRI in fourteen patient-derived realistic lead models: The role of extracranial lead management," *Proc. Intl. Soc. Magn Reson Med* 25 2017.

[14] E. Kazemivalipour et al., "Reconfigurable MRI technology for low-SAR imaging of deep brain stimulation at 3T: Application in bilateral leads, fully-implanted systems, and surgically modified lead trajectories," *NeuroImage*, vol. 199, pp. 18-29, 2019.

[15] B. T. Nguyen, B. Bhusal, and L. Golestanirad, "Interdependency of SAR amplification on external trajectory and internal geometry of implanted leads during MRI at 3T," *Proc. Intl. Soc. Magn Reson Med* 28 2020.

[16] L. Golestanirad *et al.*, "Reconfigurable MRI coil technology can substantially reduce RF heating of deep brain stimulation implants: First in-vitro study of RF heating reduction in bilateral DBS leads at 1.5 T," *PloS one,* vol. 14, no. 8, 2019.